

Modeling of the Wegener–Bergeron–Findeisen process—implications for aerosol indirect effects

T Storelvmo¹, J E Kristjánsson², U Lohmann¹, T Iversen³,
A Kirkevåg³ and Ø Seland³

¹ Institute for Atmospheric and Climate Sciences, ETH Zurich, Zurich, Switzerland

² Department of Geosciences, University of Oslo, Oslo, Norway

³ Norwegian Meteorological Office, Oslo, Norway

E-mail: trude.storelvmo@env.ethz.ch

Received 14 January 2008

Accepted for publication 20 August 2008

Published 8 October 2008

Online at stacks.iop.org/ERL/3/045001

Abstract

A new parameterization of the Wegener–Bergeron–Findeisen (WBF) process has been developed, and implemented in the general circulation model CAM-Oslo. The new parameterization scheme has important implications for the process of phase transition in mixed-phase clouds. The new treatment of the WBF process replaces a previous formulation, in which the onset of the WBF effect depended on a threshold value of the mixing ratio of cloud ice. As no observational guidance for such a threshold value exists, the previous treatment added uncertainty to estimates of aerosol effects on mixed-phase clouds. The new scheme takes subgrid variability into account when simulating the WBF process, allowing for smoother phase transitions in mixed-phase clouds compared to the previous approach. The new parameterization yields a model state which gives reasonable agreement with observed quantities, allowing for calculations of aerosol effects on mixed-phase clouds involving a reduced number of tunable parameters. Furthermore, we find a significant sensitivity to perturbations in ice nuclei concentrations with the new parameterization, which leads to a reversal of the traditional cloud lifetime effect.

Keywords: aerosols, mixed-phase clouds, microphysics

1. Introduction

In recent years, aerosol–cloud interactions have been studied extensively in laboratories, in models, in dedicated field campaigns and using satellite data. As a result of this effort, our understanding of aerosol–cloud interactions has increased, and so has the number of hypotheses on how anthropogenic aerosols can potentially influence clouds (Lohmann and Feichter 2005). Some of these mechanisms are relatively well understood and accepted by the scientific community, whereas others are more uncertain.

Anthropogenic aerosols influence clouds differently depending on the thermodynamic state of the cloud, i.e. whether it consists of liquid only (warm clouds), both ice crystals and cloud droplets (mixed-phase clouds) or ice

only (cirrus clouds). For warm clouds, anthropogenic aerosols increase the cloud albedo by acting as cloud condensation nuclei (CCN), thereby decreasing cloud droplet sizes (Twomey 1977). The level of scientific understanding of this process was upgraded from ‘very low’ in the third assessment report (TAR) by the Intergovernmental Panel for Climate Change (IPCC) to ‘low’ in the fourth assessment report (AR4) by the IPCC (Forster *et al* 2007). The anthropogenic decrease in cloud droplet sizes can in some cases lead to less efficient precipitation production, which in turn can lead to increased cloud lifetimes (Albrecht 1989). This effect is still associated with a ‘very low’ level of understanding (Denman *et al* 2007). Clearly, there is still room for progress in the understanding of aerosol effects on warm clouds. Aerosol effects on mixed-phase clouds are less well understood, and it is still not clear

if anthropogenic aerosols affect them. Ice formation in these clouds always occurs by the aid of so-called ice nuclei (IN), i.e. by heterogeneous freezing. The freezing mechanisms most relevant in the context of this paper are contact freezing (freezing of a supercooled droplet subsequent to an ice nucleus coming into contact with it) and immersion freezing (freezing of a supercooled droplet by an ice nucleus suspended in the body of water). For an overview of the different heterogeneous ice nucleation modes, see e.g. Vali (1985), and for *in situ* measurements of heterogeneous freezing, see e.g. DeMott *et al* (2003). IN are typically insoluble particles, sometimes with crystalline structure, candidates being mineral dust, biological particles and soot (Pruppacher and Klett 1997). Soot particles are largely of anthropogenic origin, so if they are in fact efficient IN, anthropogenic activity has introduced additional IN into the atmosphere. Such an increase in IN would lead to an anthropogenic increase in freezing and cloud glaciation. This effect has been referred to as the *cloud glaciation effect* (Lohmann 2002). Conversely, anthropogenic sulfur coatings can potentially deactivate the IN (Girard *et al* 2004), or alternatively make them less efficient in relatively warm mixed-phase clouds (Storelvmo *et al* 2008, Hoose *et al* 2008). This complete or partial deactivation will hereafter be referred to as the *deactivation effect*. Additionally, as large droplets freeze more readily than small droplets (Pruppacher and Klett 1997), the anthropogenic decrease in cloud droplet radius would be expected to counteract freezing. This effect has been termed the *thermodynamic effect*, and has been discussed by, for example, Rosenfeld and Woodley (2000). All in all, it is far from obvious what the net anthropogenic aerosol effect on mixed-phase clouds is.

The formation of pure ice clouds (i.e. cirrus) by homogeneous freezing of supercooled aerosols may occur at temperatures below approximately -35°C (Koop 2004). However, the presence of IN may delay or entirely prevent homogeneous freezing, as heterogeneous freezing processes may deplete water vapor to the extent that the high supersaturations ($\sim 170\%$) required for the onset of homogeneous freezing are never obtained (e.g. DeMott *et al* 1997). This competition between homogeneous and heterogeneous freezing processes is not yet fully understood (e.g. Gierens 2003), and how the IN get transported to sufficiently high altitudes and in high enough concentrations to have an impact are also issues requiring further research.

In this paper we focus on the Wegener–Bergeron–Findeisen process and its importance for aerosol indirect effects associated with stratiform mixed-phase clouds. We study these effects in the CAM-Oslo general circulation model (GCM) with an extended mixed-phase cloud microphysics scheme taking the three mechanisms mentioned above (the *glaciation*, *deactivation* and *thermodynamic* effects) into account. In this microphysics scheme, we recently implemented a new parameterization of the Wegener–Bergeron–Findeisen (WBF) process, based on a derivation presented in Korolev (2007). The WBF process refers to the rapid growth of ice crystals at the expense of cloud droplets (at temperatures below 0°C and above approximately -35°C) due to the difference in saturation vapor pressure over water

compared to that over ice. So far, this process has typically not been accounted for in general circulation models (GCMs), as various forms of interpolation have been used to specify the liquid fraction of a cloud at temperatures below freezing (Rasch and Kristjánsson 1998, Lohmann and Roeckner 1996). In recent years, some GCM studies have accounted for the WBF process in a simplistic manner, by assuming that when a critical cloud ice mixing ratio is reached the entire cloud glaciates (Lohmann and Diehl 2006, Storelvmo *et al* 2008). Glaciation drastically changes cloud radiative properties and precipitation release. There is currently no observational support or guidance for such a critical ice mixing ratio approach. Clearly, a process so crucial for cloud radiative and microphysical properties calls for a less crude approach. The purpose of the paper is to present a new parameterization which attempts to treat the WBF process in a physically more realistic manner, taking the subgrid variation in vertical velocity and hence relative humidity into account. A simplified subgrid treatment of the WBF process has previously been employed by Rotstain (1997). Based on a single-moment cloud microphysics scheme and a triangular probability density function for the total water mixing ratio, the fraction of a cloud where ice and liquid can co-exist was calculated. In this study, we advance the subgrid approach further by explicitly accounting for heterogeneous freezing processes, which are crucial for the onset and progress of the WBF process. Furthermore, a double-moment cloud microphysics scheme and a subgrid treatment of vertical velocity allows for the use of the theoretically based treatment of the WBF process presented in Korolev (2007) and Korolev and Mazin (2003).

In the following section, our modeling framework CAM-Oslo will be described. Thereafter, we will give an overview of the mixed-phase cloud microphysics scheme and the details of the new WBF parameterization. The results from CAM-Oslo with and without aerosol effects on mixed-phase clouds (experiments AER_{MIX} and AER_{LIQ}, respectively), and with the new WBF parameterization (experiment AER_{WBF}) will be presented in section 3. A discussion of the results, along with conclusions and suggestions for future work, is given in section 4.

2. Description of CAM-Oslo and the new WBF parameterization

2.1. CAM-Oslo

The CAM-Oslo GCM is an extended version of the National Center for Atmospheric Research (NCAR) Community Atmosphere Model Version 3 (CAM3) (Collins *et al* 2006). For this study the simulations were carried out with an Eulerian dynamical core at T42 spectral truncation, which corresponds to a horizontal gridspacing of $2.8^{\circ} \times 2.8^{\circ}$ on a Gaussian grid. There are 26 levels in the vertical, out of which approximately half are located in the troposphere. The vertical layer thickness ranges from a few hundred metres near the surface to more than 1 km in the upper troposphere. The stratiform cloud microphysics scheme used in CAM3 was developed by Rasch and Kristjánsson (1998). To form CAM-Oslo, CAM3 has been extended with a framework for calculations of aerosol direct

and indirect effects on climate. The framework is developed by the aerosol and cloud researchers at the University of Oslo and the Norwegian Meteorological Institute, and consists of the following components:

- *An aerosol life cycle scheme* treating the life cycle of five aerosol components and two aerosol precursor gases in the atmosphere. The components treated are: (i) sea salt, (ii) mineral soil dust, (iii) black carbon (BC), (iv) particulate organic matter, (v) particulate sulfate, (vi) di-methyl-sulfide (DMS), and (vii) sulfur dioxide. The preindustrial (PI) and present day (PD) emissions of these components are taken from Dentener *et al* (2006) and used in the AeroCom project. The scheme accounts for sulfuric acid gas condensation onto preexisting particles, coagulation in clear and cloudy air, wet phase chemical processes in clouds, new particle formation, and dry and wet deposition. For more detail, see Seland *et al* (2008).
- *A scheme calculating aerosol size distribution and optical properties* treating internal and external aerosol mixing. All primary particles are represented by a superposition of multiple lognormal modes. This multimodal lognormal size distribution is then modified by the processes mentioned above and by hygroscopic growth, the modifications being described by 44 logarithmically spaced size-bins in the radius range 0.001–20 μm . Aerosol direct radiative effects are calculated using precalculated look-up tables to calculate aerosol optical properties based on Mie theory (Seland *et al* 2008).
- *A scheme calculating aerosol effects on warm clouds* based on a double-moment liquid cloud microphysics scheme, i.e. it includes prognostic equations for both the cloud liquid water mixing-ratio and cloud droplet number concentration (based on Storelvmo *et al* 2006). Cloud droplet activation is calculated based on a subgrid distribution of vertical velocity and hence supersaturation, employing the scheme of Abdul-Razzak and Ghan (2000). The lowering of supersaturation at high CCN concentrations (the so-called competition effect) is accounted for.
- *A scheme calculating aerosol effects on mixed-phase clouds* based on a double-moment ice microphysics scheme (i.e. a prognostic treatment of both cloud ice mixing ratio and ice crystal number concentration). The scheme accounts for heterogeneous freezing via the contact and immersion/condensation freezing modes, precipitation release through the ice phase, ice multiplication processes, melting and sublimation. Mineral dust and BC are the two ice nucleating aerosol species in the model. Their zonally and annually averaged number concentrations for present day emissions are shown in figures 1(a) and (b), respectively. The BC number concentrations are significantly higher than the mineral dust number concentrations, but they initiate freezing at substantially lower temperatures. Heterogeneous freezing processes are calculated based on the parameterization presented in Lohmann and Diehl (2006) and described in detail in Storelvmo *et al* (2008).

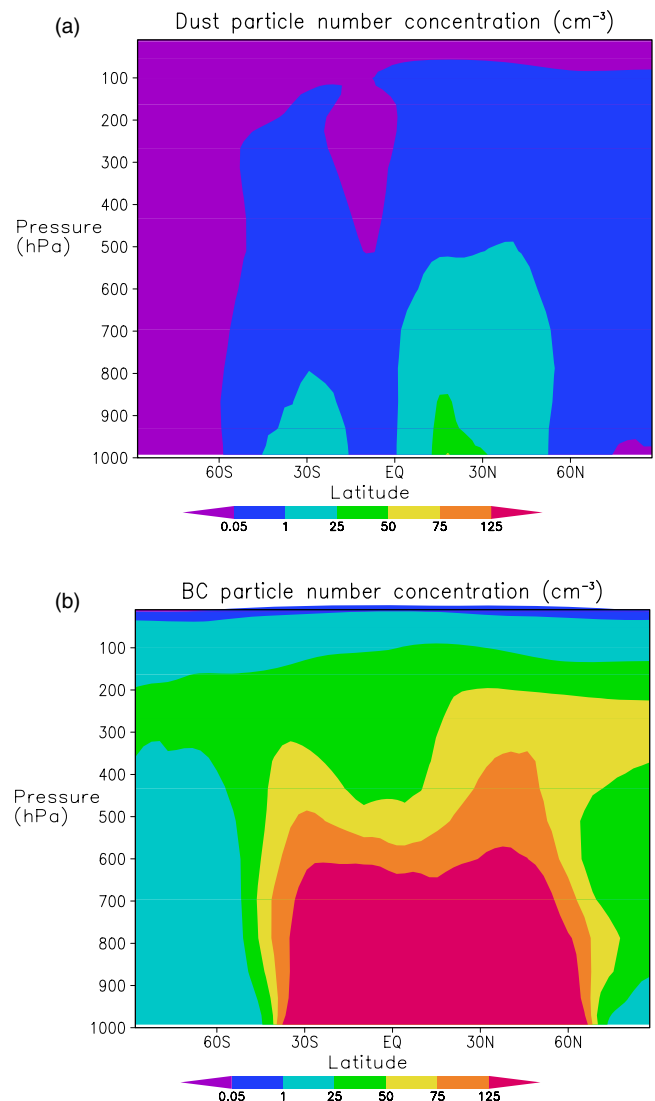


Figure 1. Annually and zonally averaged number concentrations of (a) mineral dust and (b) BC, simulated for present day emissions.

The formation of cirrus clouds, i.e. clouds forming at temperatures below -35°C , remains unchanged in this study; hence it is treated as in NCAR CAM3 and is not influenced by aerosols. We will discuss this issue further in section 4.

2.2. The mixed-phase cloud microphysics scheme with the new treatment of the WBF process

In this section we present the novel treatment of the WBF process in the model, which employs the equations presented by Korolev and Mazin (2003). In Korolev (2007) it is pointed out that the WBF process can only occur in a limited range of conditions, and that one cannot automatically apply it to all mixed-phase clouds, which is currently a common modeling approach. The relationship between (i) the in-cloud vapor pressure (e), (ii) the saturation vapor pressure over liquid water (e_s), and (iii) the saturation vapor pressure over ice (e_i) determines the growth/evaporation of cloud droplets and ice

crystals. For mixed-phase clouds, there are three possible regimes:

- *Regime 1*—Both droplets and ice crystals grow simultaneously. For a given cloud or cloud fraction, this occurs when the following is true:

$$e > e_s > e_i. \quad (1)$$

It was shown by Korolev and Mazin (2003) that this may occur if the updraft velocity u_z is higher than a critical updraft velocity, u_z^* given by

$$u_z^* = \frac{e_s - e_i}{e_i} N_i \bar{r}_i \eta \quad (2)$$

where η is a coefficient dependent on temperature (T) and pressure (p), N_i is the ice crystal number concentration and \bar{r}_i is the mean volume radius of the ice particles ($\bar{r}_i = (\frac{3IWC}{4\pi N_i \rho_i})^{\frac{1}{3}}$, where IWC is the cloud ice water content and ρ_i is the density of ice.). For regime 1 conditions, the mixed phase is maintained for an indefinite period, as long as (1) holds.

- *Regime 2*—Ice crystals grow at the expense of cloud droplets (WBF process). The WBF process takes place if the following requirement is fulfilled:

$$e_s > e > e_i. \quad (3)$$

If (3) is true, cloud droplets will inevitably evaporate, providing a source of water vapor for depositional growth of ice crystals. A cloud or cloud fraction in regime 2 will eventually glaciate, the glaciation timescale being dependent on the ice crystal number, ice water content (IWC) and liquid water content (LWC), among others. From Korolev and Mazin (2003), (3) is fulfilled if

$$u_z^0 < u_z < u_z^* \quad (4)$$

where u_z^0 is the negative vertical velocity below which ice crystals will sublimate rather than grow:

$$u_z^0 = \frac{e_i - e_s}{e_s} N_w \bar{r}_w \chi \quad (5)$$

where χ is a coefficient dependent on p and T , and N_w and \bar{r}_w are the cloud droplet number concentration and cloud droplet mean volume radius, respectively ($\bar{r}_w = (\frac{3LWC}{4\pi N_w \rho_w})^{\frac{1}{3}}$, where ρ_w is the density of water).

- *Regime 3*—Both ice crystals and droplets evaporate simultaneously. A cloud or cloud fraction falls in regime 3 in the case of

$$e_s > e_i > e. \quad (6)$$

According to Korolev and Mazin (2003), (6) is true in downdrafts when $u_z < u_z^0$.

In CAM-Oslo, a subgrid distribution of vertical velocity is already implemented for calculations of cloud droplet activation. The same distribution is now used to determine the fractions of a given cloud dominated by each of the three regimes outlined above. The subgrid vertical velocity

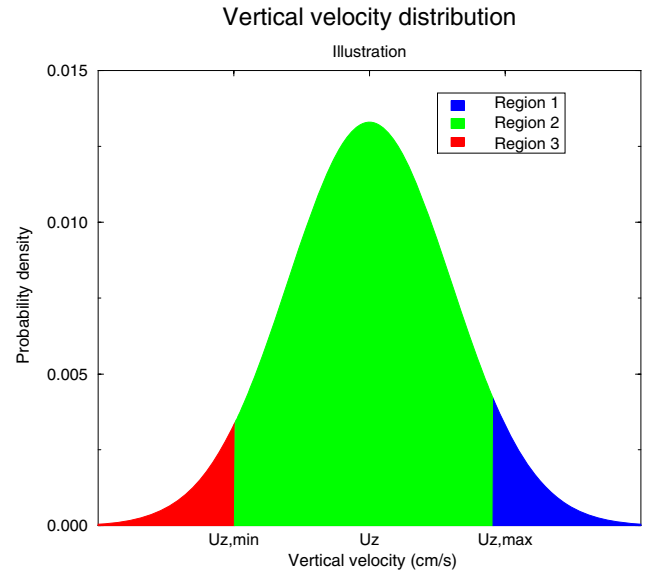


Figure 2. Illustration of the subgrid vertical velocity distribution, with shadings indicating typical but fictive grid box fractions dominated by regime 1 (blue shading), regime 2 (green shading) and regime 3 (red shading), respectively.

distribution is described by a Gaussian normal distribution centered around the mean grid box vertical velocity \bar{u}_z , following the parameterization of Ghan *et al* (1997). The width of the distribution is given by the standard deviation (σ_{u_z}), calculated as follows:

$$\sigma_{u_z} = \frac{\sqrt{2\pi K}}{\Delta z} \quad (7)$$

where K is the vertical eddy diffusivity and Δz is the model layer thickness. As the relatively coarse resolution of the model may lead to an underestimation of σ_w , a lower limit of 0.30 ms^{-1} is necessary. Figure 2 gives an illustration of the subgrid vertical velocity distribution, indicating typical but idealized grid box fractions dominated by regimes 1, 2 and 3, respectively.

The rates of condensation, evaporation, deposition and sublimation are determined in the model using a so-called saturation adjustment approach. This implies that any supersaturation is immediately removed by condensation and/or deposition of the excess water vapor. Similarly, subsaturations in the presence of cloud condensate will immediately lead to evaporation and/or sublimation until saturation is reached or all cloud condensate is depleted. In regime 1, the saturation adjustment is calculated with respect to liquid water, whereas in regimes 2 and 3 the adjustment is carried out with respect to ice, as supported by Korolev and Isaac (2008).

3. Experimental setup and results

In the following sections we present the results from three model experiments. Each experiment is a twin simulation, one with present day (PD) aerosol emissions and the other with aerosol emissions corresponding to preindustrial (PI)

conditions. All simulations use climatological sea surface temperatures and are run for 5 years after a model spin-up of 4 months. An overview and a short description of the three experiments are given in table 1. Global and annual averages of cloud radiative and microphysical properties for the simulations are presented in table 2, and anthropogenic changes in cloud and radiation variables (calculated by subtracting the value from the PI simulation from that of the PD simulation) are given in table 3. Aerosol optical properties are as in the standard NCAR CAM3 model, and are the same for all simulations. Hence, no direct aerosol effects are included in the simulations.

3.1. Experiment AER_{LIQ}

This simulation accounts for aerosol effects on liquid clouds only, whereas ice clouds are not influenced by aerosols other than indirectly through their interactions with liquid clouds. The aerosol effect on liquid clouds is calculated mainly as in Storelvmo *et al* (2006), employing a continuity equation for cloud droplet number concentration. The source term in this continuity equation is calculated using the cloud droplet activation scheme developed by Abdul-Razzak and Ghan (2000), and we account for microphysical cloud droplet sinks like evaporation, freezing, precipitation and self-collection. Important changes from Storelvmo *et al* (2006) are as follows. (1) The aerosol scheme has changed drastically, and now predicts mineral dust and sea salt mass and number concentrations rather than prescribing them. The modal radius for accumulation mode mineral dust is increased from 0.088 to 0.22 μm , which reduces the mineral dust number concentration substantially, thereby reducing the amount of natural CCN and IN in the model. For more detail, see Seland *et al* (2008). (2) The host model in Storelvmo *et al* (2006) was NCAR CAM version 2 (CAM2, <http://www.cesm.ucar.edu/models/atm-cam/docs/cam2.0/>), while the current version of CAM-Oslo is based on NCAR CAM3 (Collins *et al* 2006). In CAM3, cloud condensate is transported not only vertically (as in CAM2), but also horizontally. Consequently, cloud droplets are also transported horizontally for consistency. Additionally, in CAM3, all cloud condensate remains liquid at temperatures down to -10°C , and thereafter the cloud ice fraction increases linearly with decreasing temperatures and reaches unity at -40°C . In CAM2, the ice fraction starts to increase as soon as temperatures drop below 0°C , and reaches unity at -20°C .

The new treatment of sea salt and mineral dust aerosols has reduced the mass and number burdens of these natural aerosols substantially. Menon *et al* (2002) found the aerosol indirect effect (AIE) to be extremely sensitive to the PI aerosol burden, and discussed how a decrease in the PI aerosol burden can substantially strengthen the AIE. This was recently supported by the findings of Kirkevåg *et al* (2008). As a consequence of the reduced natural aerosol concentration, the aerosol indirect effect is increased in this study as compared to Storelvmo *et al* (2006). The globally averaged change in the net cloud forcing (NCF) at the top of the atmosphere (TOA) due to anthropogenic aerosols is -1.50 W m^{-2} here (alternatively -1.93 W m^{-2} when calculated as a change in

Table 1. Sensitivity simulations.

Simulation	Description
AER_{LIQ}	Simulation including aerosol effects on liquid clouds only
AER_{MIX}	As AER_{LIQ} , but also including aerosol effects on mixed-phase clouds
AER_{WBF}	As AER_{MIX} , but including the new parameterization of the WBF process

the net radiative flux at the TOA), compared to the range -0.13 to -0.72 W m^{-2} in Storelvmo *et al* (2006). Yet another factor contributing to the increased aerosol indirect effect is the low minimum value for cloud droplet number concentration (CDNC) applied in this study (0.1 cm^{-3} compared to 10 cm^{-3} in Storelvmo *et al* (2006)). Such minimum CDNC values are frequently used in studies of aerosol indirect effects in global models, and act to artificially reduce the AIE.

3.2. Experiment AER_{MIX}

In this experiment, heterogeneous freezing processes initiated by soot and mineral dust are accounted for (in a similar way as in experiment AIE_mono in Storelvmo *et al* (2008)). Mineral dust and soot particles act as immersion ice nuclei (i.e. freezing cloud droplets from within) when internally mixed or coated with soluble material, and as contact ice nuclei (i.e. freezing cloud droplets upon contact) when externally mixed or uncoated. Freezing efficiencies for soot and mineral dust in the contact and immersion mode are taken from the compilation by Diehl *et al* (2006), and the heterogeneous freezing rates are calculated as in Lohmann and Diehl (2006). The ice fraction of the cloud condensate is no longer determined by temperature alone (as in AER_{LIQ}), but rather is a result of the freezing/melting processes taking place in the model. Both in this experiment and in experiment AER_{WBF} , mineral dust particles are assigned the freezing properties of montmorillonite, a relatively efficient ice nucleus. This simplification is justified by a study by Hoose *et al* (2008), where the assumption that all mineral dust consists of montmorillonite gives similar results to simulating a realistic dust mineralogy. The three mechanisms through which aerosols can influence mixed-phase clouds (as described in section 1), are all taken into account in this experiment.

As seen from table 2, the liquid water path (LWP) is lower in this simulation compared to simulation AER_{LIQ} , because cloud liquid water may now freeze even at relatively warm temperatures as long as IN are available. However, as the WBF process glaciates the entire grid box as soon as a critical ice mixing ratio ($10^{-5}\text{ kg kg}^{-1}$) is reached, precipitation release becomes efficient and most of the frozen cloud water is efficiently converted into precipitation rather than remaining in the atmosphere as cloud ice. Hence, the ice water path (IWP) is increased compared to AER_{LIQ} , but this increase is much smaller than the LWP decrease. An increase in the stratiform precipitation rate compared to AER_{LIQ} supports the reasoning above, but is compensated by a reduction in convective precipitation. As seen from table 3, introducing heterogeneous freezing processes leads to

Table 2. Modeled and observed annual global mean cloud microphysical and radiative properties. Total cloud cover observations are obtained from surface observations (Hahn *et al* 1994), the International Satellite Cloud Climatology Project (ISCCP) (Rossow and Schiffer 1999) and MODIS data (King *et al* 2003). The LWP observations are from SSM/I (Ferraro *et al* 1996, Greenwald *et al* 1993, Weng and Grody 1994) and the ice water path (IWP) is derived from ISCCP data (Storelvmo *et al* 2008). The shortwave and longwave cloud forcing (SWCF and LWCF) estimates are from Kiehl and Trenberth (1997), and the effective droplet radius observations are from Han *et al* (1994).

Simulation	AER _{LIQ}	AER _{MIX}	AER _{WBF}	Observations
Cloud cover (%)	60.0	61.7	64.1	62–67
Liquid water path (g m ⁻²)	131.3	86.3	99.2	50–84
Ice water path (g m ⁻²)	17.0	25.9	32.9	29.4
SWCF, TOA (W m ⁻²)	-54.4	-43.8	-50.4	-50
LWCF, TOA (W m ⁻²)	29.5	28.1	31.8	30
Effective droplet radius (μm)	13.7	13.9	14.0	11.4
Total precipitation (mm/day)	2.84	2.80	2.77	2.74
Convective precipitation (mm/day)	2.06	1.82	1.83	—
Stratiform precipitation (mm/day)	0.77	0.98	0.93	—

a smaller anthropogenic increase in the amount of shortwave radiation reflected back to space compared to AER_{LIQ}. This is due to the smaller anthropogenic increase in LWP in this experiment (reduced by about 30% compared to AER_{LIQ}). However, this LWP reduction also allows more longwave radiation to be transmitted to space, leading to an aerosol indirect effect (i.e. a reduction in net radiation at the TOA) which is only slightly reduced compared to AER_{LIQ}. As we will demonstrate, this finding is very sensitive to the treatment of the WBF process in this experiment.

3.3. Experiment AER_{WBF}

In this experiment, the new parameterization of the WBF process as described in section 2.2 is included. Rather than imposing an abrupt cloud glaciation of the entire grid box, the new approach mimics a subgrid scale process in which the WBF process can be initiated in a small fraction of the grid box, leading to fractional glaciation. Typically, the cloud fraction in which the WBF process takes place (region 2 in figure 2) will expand as ice particles form and grow. This follows from equation (2), and the physical reasoning is that if ice crystals are present in high concentrations, water vapor will be efficiently depleted and the cloudy air will be subsaturated with respect to liquid droplets.

Figures 3(a)–(c) show the zonally and annually averaged cloud fractions dominated by the three regimes depicted in figure 2. Values are only sampled for temperatures between 0 and -35 °C, and only when clouds are present in a grid box. Figure 3(a) shows the fraction of the cloud where updraft velocities are large enough to allow both ice crystals and cloud droplets to grow simultaneously. As expected, this fraction is large in relatively warm mixed-phase clouds (i.e. at low latitudes and altitudes) where the ice crystal production is relatively low. The few ice crystals formed are not able to deplete the available water vapor, and droplets may grow. This fraction of the cloud is also expected to be large in regions associated with high vertical velocities (e.g. in connection to the Hadley circulation in the tropics or in connection to the polar frontal systems). Additionally, the term $\frac{e_s - e_i}{e_i}$ in equation (2) becomes small in warm mixed-phase clouds, i.e. at low altitudes/latitudes, which leads to an increase in this cloud fraction. Based on the reasoning above,

Table 3. Annual global mean changes in cloud microphysical and radiative properties from preindustrial to present day.

Simulation	AER _{LIQ}	AER _{MIX}	AER _{WBF}
Cloud cover (%)	-0.21	-0.21	-0.25
Liquid water path (g m ⁻²)	5.4	4.1	-6.9
Ice water path (g m ⁻²)	0.17	-0.28	0.20
Shortwave radiation, TOA (W m ⁻²)	-1.66	-1.11	1.13
Outgoing longwave radiation (W m ⁻²)	-0.27	-0.38	-1.08
Net radiation, TOA (W m ⁻²)	-1.93	-1.49	0.05
Effective droplet radius (μm)	-0.96	-1.01	-0.89
Precipitation (mm/day)	-0.004	-0.026	0.011

the fraction of the cloud where the WBF process takes place (i.e. where ice crystals grow at the expense of cloud droplets) is larger in colder mixed-phase clouds, as shown in figure 3(b). Finally, the fraction of the cloud where both ice crystals and cloud droplets evaporate/sublimate (figure 3(c)) is significantly smaller than those dominated by the other two regimes. It reaches non-negligible values only in downdraft regions with low droplet concentrations (i.e. at high latitudes and altitudes), in agreement with equation (5). From the same equation, it can be seen that when the term $\frac{e_i - e_s}{e_s}$ becomes small (at warm temperatures, i.e. at low altitudes and latitudes), this fraction of the cloud becomes larger.

The cloud fraction in which the WBF process takes place (i.e. where cloud glaciation occurs) is systematically larger (by 3 to 10%) at all model levels in the PD simulation compared to the PI case. The significantly higher number concentrations of soot in the PD simulations lead to increased heterogeneous freezing (mainly contact freezing) and higher ice crystal number concentrations in the PD case. According to equation (2), this ice crystal production leads to an expansion of the glaciating fraction of the cloud, and hence an increase in ice water content and reduction in liquid water content. As a consequence, table 3 shows a strong anthropogenic decrease in the LWP and an increase in the IWP for this experiment, leading to a reversal of the traditional cloud lifetime effect. As is evident from figure 4(a), the anthropogenic increase in the IWP is mainly due to an increased ice water content in relatively warm mixed-phase clouds, where contact freezing

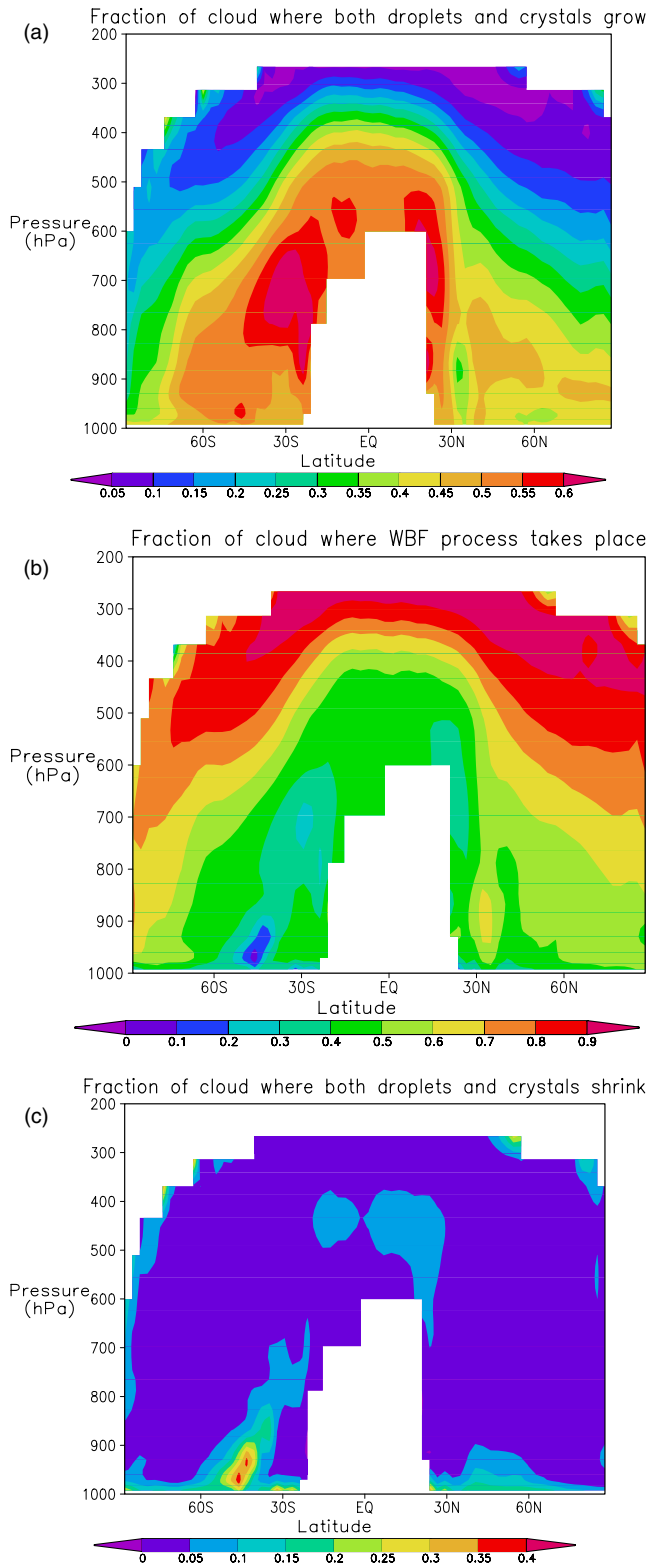


Figure 3. Simulated cloud fractions dominated by (a) regime 1 (i.e. simultaneous growth of droplets and ice crystals), (b) regime 2 (i.e. ice crystal growth at the expense of cloud droplets), and (c) regime 3 (i.e. sublimation of ice crystals and evaporation of cloud droplets).

is the dominant heterogeneous freezing process. Figure 4(b) shows the corresponding anthropogenic reduction in the LWC for mixed-phase clouds, while at levels dominated by liquid

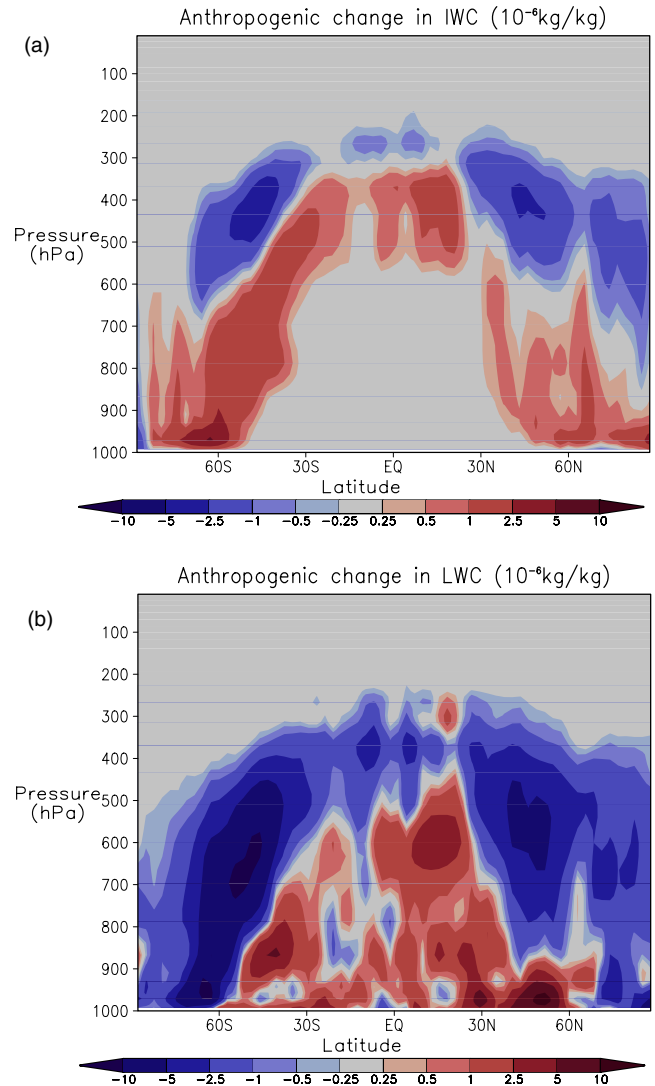


Figure 4. Zonally averaged anthropogenic change in (a) ice water content (kg kg^{-1}) and (b) liquid water content (kg kg^{-1}), both from the simulation AER_{WBF} , calculated by subtracting the PI values from the PD values.

clouds the LWC is increased, as expected from the traditional lifetime effect for liquid clouds. As a consequence of these significant changes in cloud condensate, the radiation balance is now significantly altered. The anthropogenic change in shortwave radiation at the TOA is now positive, as the reversed cloud lifetime effect leads to a reduction in the shortwave radiation reflected back to space. Similarly, more longwave radiation is now transmitted through the clouds, leading to a negative change in the longwave radiation at the TOA. The net change in radiation at the TOA amounts to 0.05 W m^{-2} . This result is intriguing, as the vast majority of global models simulating the aerosol indirect effect find it to be negative. It seems clear that a much stronger anthropogenic effect on mixed-phase clouds is possible when the WBF process is treated in a more physical manner, where a smoother transition from liquid to ice phase allows for a larger difference between cases with and without abundant IN concentrations. We will discuss this somewhat surprising result further in the following section.

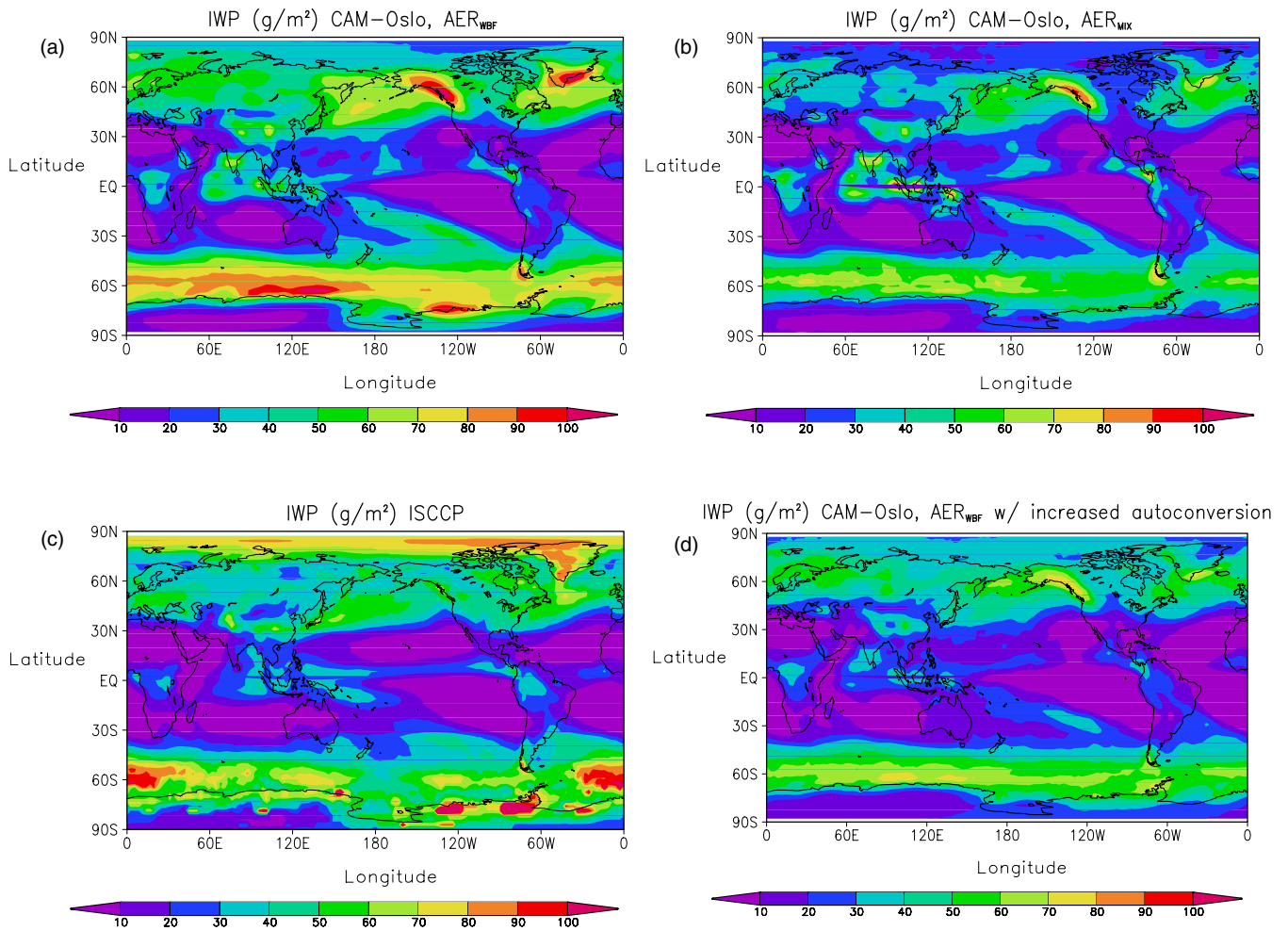


Figure 5. Ice water path (IWP) (g m^{-2}) (a) as simulated with CAM-Oslo with new WBF scheme included, (b) simulated with CAM-Oslo with old treatment of the WBF process, (c) from the ISCCP dataset (Rossow and Schiffer 1999), and (d) simulated with CAM-Oslo with new WBF scheme and reduced threshold for onset of autoconversion in cold clouds.

With the previous treatment of the WBF process (as in AER_{MIX}), a cloud could remain mainly liquid at very low temperatures as long as the critical ice mixing ratio for initiation of the WBF process was not obtained. Here, as soon as very small amounts of ice have formed, glaciation can slowly begin. Consequently, the IWP is increased in this experiment compared to AER_{MIX} (see table 2). Figures 5(a)–(c) show the IWP from this experiment compared to the IWP from experiment AER_{MIX} and to satellite observations from the International Satellite Cloud Climatology Project (ISCCP). The spatial distributions of the modeled IWPs are in good agreement with satellite observations, whereas quantitatively AER_{MIX} underestimates the IWP while AER_{WBF} overestimates the IWP in the storm tracks in both hemispheres. While the globally averaged shortwave cloud forcing (SWCF) of experiment AER_{WBF} is in excellent agreement with satellite observations, the longwave cloud forcing (LWCF) is on the high side, probably partly due to the overestimated IWP. There are several possible explanations for this overestimation, which will be discussed further in section 4.

4. Discussion and conclusion

A new treatment of the Wegener–Bergeron–Findeisen (WBF) process has been implemented in the CAM-Oslo GCM, providing a theoretically based treatment of cloud glaciation. The new WBF treatment yields smoother transitions from liquid to ice in clouds with cloud temperatures from -35 to 0°C than the earlier treatment. Previously, glaciation occurred abruptly when a critical ice mixing ratio was obtained (Storelvmo *et al* 2008). Applying such a sudden glaciation to a cloud extending horizontally over hundreds of square kilometres is not physically realistic. Furthermore, as no observational guidance exists as to what such a critical ice mixing ratio should be, the previous approach added a free parameter and therefore uncertainty to climate simulations. We have shown that the new approach yields physically sound results and allows for much stronger aerosol effects on mixed-phase clouds, counteracting the aerosol effects on warm clouds and yielding a change in net radiation at the top of the atmosphere (i.e. a measure of the aerosol indirect effect) of 0.05 W m^{-2} when aerosol effects on both liquid and mixed-phase clouds are accounted for. As a reference,

accounting only for aerosol effects on warm clouds gives a change in net radiation at the TOA of -1.93 W m^{-2} , while the earlier treatment of WBF gives a change of -1.49 W m^{-2} (table 3). The results rely heavily on the heterogeneous freezing efficiencies for various aerosol types given in Diehl *et al* (2006), and could be quite different for other freezing efficiencies. Similarly, a different aerosol scheme yielding different BC and mineral dust concentrations could also lead to different results. Hence, we hesitate to make firm conclusions regarding the sign of the aerosol indirect effect based on the somewhat surprising result in simulation AER_{WBF}. However, we can safely conclude that the new treatment of the WBF process allows for much stronger responses to changes in IN concentrations than found in most previous studies. A recent study by Xie *et al* (2008) also found cloud properties in two global models to be very sensitive to the treatment of the WBF process, although aerosol indirect effects were not calculated. One of these models was, as CAM-Oslo, based on the NCAR CAM3 model, but with extensions to the cloud microphysics described in Liu *et al* (2007).

With the new WBF treatment, annually averaged IWPs observed by satellite are overall reproduced satisfactorily. However, we note an overestimation of the IWP in the midlatitude storm tracks. We suggest the following three possible explanations for this overestimation. (1) The precipitation release via the ice phase may not be efficient enough. This would show up as an IWP overestimation especially in the storm tracks, where precipitation formation plays a major role. The autoconversion process for ice is described in Rasch and Kristjánsson (1998) by a rate term multiplied by a threshold term. When a temperature-dependent threshold for the ice mixing ratio is exceeded, the autoconversion of ice is initiated. As ice crystals in mixed-phase clouds will almost invariably grow large enough to fall out as precipitation, this threshold approach may not be a realistic one. Figure 5(d) shows the IWP from a sensitivity simulation identical to AER_{WBF} (with PD emissions), but with a slight reduction in the autoconversion threshold for mixed-phase clouds. Evident is the pronounced IWP reduction in the midlatitude storm tracks. Hence, improving the treatment of autoconversion in the model and removing such unphysical thresholds is likely to have a large effect on the IWP in mid latitudes. A reformulation of the autoconversion process for ice is beyond the scope of this paper, but will be the subject of future studies. (2) An underestimation of the entrainment and mixing with out-of-cloud dry air near cloud boundaries could lead to simultaneous evaporation of ice crystals and cloud droplets, although the downdraft velocity is not below the critical value given by equation (5). The generally poor treatment of such processes in GCMs has been pointed out by, for example, Wood (2006), and could in some cases lead to overestimations of cloud water and ice content. (3) The normal distribution assumed for the vertical velocity within a grid box may not represent the real vertical velocity well, especially not for typical storm track clouds. The literature suggests that different vertical velocity distributions may be appropriate for different cloud types. For instance, for cirrus clouds there is some support

in the literature for a normal distribution (Quante 2006), while, for example, for orographic clouds it is suggested that the distribution should be skewed towards higher updraft velocities (supported by observations by, for example, the Swiss Meteorological Office, at the High Altitude Research Station Jungfrauoch, Switzerland). An interesting extension of the work presented here could be a sensitivity study applying other vertical velocity distributions.

Although we find that the subgrid treatment of the WBF process presented in this paper represents a step towards more realistic simulations of mixed-phase clouds in global models, we are still forced to make assumptions and simplifications that could influence our results. One example of such an assumption is that, within each grid box, cloud liquid and ice are homogeneously mixed, i.e. that clouds do not consist of separate pockets of liquid and ice. Although we subdivide clouds into three growth/evaporation regimes, the cloud fractions dominated by each of these regimes are determined from grid box cloud values. Several studies (e.g. Korolev and Isaac (2006) and Chylek and Borel (2004)) have shown that cloud phase inhomogeneities may occur, especially on scales comparable to a GCM grid box. How to represent such cloud features in global models is a challenge far beyond the scope of this paper. CAM-Oslo is currently lacking a treatment of aerosol effects on cirrus clouds, i.e. all clouds formed at temperatures below -35°C . These clouds are currently treated as in the standard NCAR CAM3, applying a saturation scheme that does not allow for the supersaturations that we know to occur at these altitudes. Including such a scheme for aerosol effects on cirrus in the future would enable CAM-Oslo to simulate aerosol–cloud interactions at all temperatures from the ground to the tropopause. Furthermore, the modeling of heterogeneous freezing processes currently suffers from large uncertainties in laboratory and *in situ* measurements of IN efficiencies for different aerosol species in the various heterogeneous freezing modes. This, and the large uncertainties associated with emission and concentrations of natural and anthropogenic IN, currently prevent modelers from being completely confident about the realism of their results.

Acknowledgments

The work presented in this paper has been supported by the Norwegian Research Council through the NORCLIM project (grant no. 178246). Furthermore, this work has received support of the Norwegian Research Council's program for Supercomputing through a grant of computer time. We are grateful to Steven Ghan at the Pacific Northwest National Laboratory for making his droplet activation scheme available and for help in implementing it in CAM-Oslo. We thank Corinna Hoose, Alexei Korolev, Andreas Mühlbauer and Peter Spichtinger for helpful comments and discussions.

References

- Abdul-Razzak H and Ghan S J 2000 A parameterization of aerosol activation, 2. Multiple aerosol type *J. Geophys. Res.* **105** 6837–44
- Albrecht B 1989 Aerosols, cloud microphysics, and fractional cloudiness *Science* **245** 1227–30

- Chylek P and Borel C 2004 Mixed phase cloud water/ice structure from high spatial resolution satellite data *Geophys. Res. Lett.* **31** L14104
- Collins W D *et al* 2006 The formulation and atmospheric simulation of the community atmosphere model version 3 (CAM3) *J. Clim.* **19** 2144–62
- DeMott P J, Cziczo D J, Prenni A J, Murphy D M, Kreidenweis S M, Thomson D S, Borys R and Rogers D C 2003 Measurements of the concentration and composition of nuclei for cirrus formation *Proc. Natl Acad. Sci. USA* **100** 14655–60
- DeMott P J, Rogers D C and Kreidenweis S M 1997 The susceptibility of ice formation in upper tropospheric clouds to insoluble aerosol components *J. Geophys. Res.* **102** 19575–84
- Denman K L *et al* 2007 Couplings between changes in the climate system and biogeochemistry *Climate Change 2007: The Physical Science Basis. Contribution of Working Group I to the Fourth Assessment Report of the Intergovernmental Panel on Climate Change* (Cambridge: Cambridge University Press)
- Dentener F *et al* 2006 Emissions of primary aerosols and precursor gases in the years 2000 and 1750 prescribed data-sets for AeroCom *Atmos. Chem. Phys.* **6** 4321–44
- Diehl K, Simmel M and Wurzler S 2006 Numerical simulations on the impact of aerosol properties and freezing modes on the glaciation, microphysics and dynamics of convective clouds *J. Geophys. Res.* **111** D07202
- Ferraro R, Weng F, Grody N and Basist A 1996 An eight year (1987–1994) time series of rainfall, clouds, water vapor, snow-cover and sea-ice derived from SSM/I measurements *Bull. Am. Meteorol. Soc.* **77** 891–905
- Forster P *et al* 2007 Changes in atmospheric constituents and in radiative forcing *Climate Change 2007: The Physical Science Basis. Contribution of Working Group I to the Fourth Assessment Report of the Intergovernmental Panel on Climate Change* (Cambridge: Cambridge University Press)
- Ghan S J, Leung L R, Easter R C and Abdul-Razzak H 1997 Prediction of cloud droplet number in a general circulation model *J. Geophys. Res.* **102** 21777–94
- Gierens K 2003 On the transition between heterogeneous and homogeneous freezing *Atmos. Chem. Phys.* **3** 437–46
- Girard E, Blanchet J-P and Dubois Y 2004 Effects of arctic sulphuric acid aerosols on wintertime low-level atmospheric ice crystals, humidity and temperature at Alert, Nunavut *Atmos. Res.* **73** 131–48
- Greenwald T J, Stephens G L, Vonder Har T H and Jackson D L 1993 A physical retrieval of cloud liquid water over the global oceans using special sensor microwave/imager (SSM/I) observations *J. Geophys. Res.* **98** 18471–88
- Hahn C J, Warren S G and London J 1994 Climatological data for clouds over the globe from surface observations 1982–1991: The total cloud edition *Tech. Rep. ORNL/CDIAC-72 NDP-026A* Oak Ridge National Laboratory, Oak Ridge, TN, USA
- Han Q, Rossow W B and Lacis A A 1994 Near-global survey of effective droplet radii in liquid water clouds using ISCCP data *J. Clim.* **7** 465–97
- Hoose C, Lohmann U, Erdin R and Tegen I 2008 Global influence of dust mineralogical composition on heterogeneous ice nucleation *Environ. Res. Lett.* **3** 025003
- Kiehl J T and Trenberth K E 1997 Earth's annual global mean energy budget *Bull. Am. Meteorol. Soc.* **78** 197–208
- King M D, Menzel W P, Kaufmann Y J, Tandre D, Gao B C, Platnick S, Ackerman S A, Remer L A, Pincus R and Hubanks P A 2003 Cloud and aerosol properties, precipitable water, and profiles of temperature and water vapor from MODIS *IEEE Trans. Geosci. Remote Sens.* **41** 442–58
- Kirkevåg A, Iversen T, Seland Ø, Debernard J B, Storelvmo T and Kristjánsson J E 2008 Aerosol–cloud–climate interactions in the climate model CAM-Oslo *Tellus A* **60** 492–512
- Koop T 2004 Homogeneous ice nucleation in water and aqueous solutions *Z. Phys. Chem.* **218** 1231–58
- Korolev A 2007 Limitations of the Wegener–Bergeron–Findeisen mechanism in the evolution of mixed-phase clouds *J. Atmos. Sci.* **64** 3372–5
- Korolev A and Isaac G A 2006 Relative humidity in liquid, mixed phase and ice clouds *J. Atmos. Sci.* **63** 2865–80
- Korolev A and Isaac G A 2008 The effect of spacial averaging on the relative humidity and phase composition of clouds *Proc. 15th Int. Conf. on Clouds and Precipitation*
- Korolev A and Mazin I P 2003 Supersaturation of water vapor in clouds *J. Atmos. Sci.* **60** 2957–74
- Liu X, Penner J E, Ghan S J and Wang M 2007 Inclusion of ice microphysics in the NCAR community atmosphere model version 3 (CAM3) *J. Clim.* **20** 4526–47
- Lohmann U 2002 Possible aerosol effects on ice clouds via contact nucleation *J. Atmos. Sci.* **59** 647–56
- Lohmann U and Feichter H 2005 Global indirect aerosol effect: a review *Atmos. Chem. Phys.* **5** 715–37
- Lohmann U and Diehl K 2006 Sensitivity studies of the importance of dust ice nuclei for the indirect aerosol effect on stratiform mixed-phase clouds *J. Atmos. Sci.* **63** 968–82
- Lohmann U and Roeckner E 1996 Design and performance of a new cloud microphysics scheme developed for the ECHAM general circulation model *Clim. Dyn.* **12** 557–72
- Menon S, Del Genio A D, Koch D and Tselioudis G 2002 GCM simulations of the aerosol indirect effect: sensitivity to cloud parameterization and aerosol burden *J. Atmos. Sci.* **59** 692–713
- Pruppacher H R and Klett J D 1997 *Microphysics of Clouds and Precipitation* 2nd edn (Norwell, MA: Kluwer–Academic)
- Quante M 2006 Turbulenz in Cirruswolken mittlerer Breiten *PhD Thesis* University of Hamburg
- Rasch P J and Kristjánsson J E 1998 A comparison of the CCM3 model climate using diagnosed and predicted condensate parameterizations *J. Clim.* **11** 1587–614
- Rosenfeld D and Woodley W L 2000 Deep convective clouds with sustained supercooled liquid water down to -37.5°C *Nature* **405** 440–2
- Rossow W B and Schiffer R A 1999 Advances in understanding clouds from ISCCP *Bull. Am. Meteorol. Soc.* **80** 2261–87
- Rotstayn L 1997 A physically based scheme for the treatment of stratiform clouds and precipitation in large-scale models. I: Description and evaluation of the microphysical processes *Q. J. R. Meteorol. Soc.* **123** 1227–82
- Seland Ø, Iversen T, Kirkevåg A and Storelvmo T 2008 Aerosol–climate interactions in the CAM-Oslo atmospheric GCM and investigation of associated basic shortcomings *Tellus A* **60** 459–91
- Storelvmo T, Kristjánsson J E and Lohmann U 2008 Aerosol influence on mixed-phase clouds in CAM-Oslo *J. Atmos. Sci.* at press doi:10.1175/2008JAS2430.1
- Storelvmo T, Kristjánsson J E, Ghan S J, Kirkevåg A, Seland Ø and Iversen T 2006 Predicting cloud droplet number concentration in community atmosphere model (CAM)-Oslo *J. Geophys. Res.* **111** D24208
- Twomey S 1977 The influence of pollution on shortwave albedo of clouds *J. Atmos. Sci.* **34** 1149–52
- Vali G 1985 Nucleation terminology *J. Aerosol. Sci.* **16** 575–6
- Weng F and Grody N C 1994 Retrieval of cloud liquid water using the special sensor microwave imager (SSM/I) *J. Geophys. Res.* **99** 25535–51
- Wood R 2006 Cancellation of aerosol indirect effects in marine stratocumulus through cloud thinning *J. Atmos. Sci.* **64** 2657–69
- Xie S, Boyle J, Klein S A, Liu X and Ghan S 2008 Simulations of Arctic mixed-phase clouds in forecasts with CAM3 and AM2 for M-PACE *J. Geophys. Res.* **113** D04211